

With respect to all inner conductors, the contours with more acute outer angles make less effective use of their perimeters, because there is more extreme concentration of current near the outer angles. By analogy with electric potential gradient, the current density is theoretically infinite at any angle whose outer side is exposed to the magnetic field. In spite of this fact, it is noted that the square suffers very little, effectively utilizing  $\pi/4$  of its perimeter. An opposite extreme is the elongated rhombus, Fig. 4(b).

Fig. 4(e) as an inner conductor might be expected to approximate the behavior of a rectangle. On the contrary, it has much less effective utilization of its contour because of the acute angles.

Referring to the more extreme shapes in Figs. 3 and 4, their equality of resistance as inner and outer conductors is remarkable and unexpected, because the current distribution is radically different in these alternative functions.

Every example of the polygon rule is an evaluation of a certain definite integral. Some of the more unusual cases may be integrals that cannot be evaluated by any procedure known to mathematicians. A long table could be prepared on the basis of this one rule.

The polygon rule offers a fascinating variety of examples based on a single theorem. It has some practical

utility in computing or estimating the skin resistance of inner and outer conductors of various polygon cross sections. Its greatest value lies in the ideas to be perceived in its examples, particularly the effect of extreme current concentration on acute angles exposed to the field. It is another interesting application of the basic "incremental-inductance rule."

#### BIBLIOGRAPHY

1. J. D. Cockroft, "Skin Effect in Rectangular Conductors at High Frequencies," *Proc. Royal Soc., (London)*, Vol. 122, (February 4, 1929), pp. 533-542. (Including square wire, in terms of elliptic integrals.)
2. H. A. Wheeler, "Formulas for the Skin Effect," *Proc. IRE*, vol. 30, (September, 1942), pp. 412-424. (The "incremental-inductance rule," derivation and applications.)
3. S. A. Schelkunoff, *Electromagnetic Waves* (New York, D. Van Nostrand and Company, 1943). (On pp. 284-285, reporting incremental-inductance rule from reference 2 above.)
4. F. E. Terman, *Radio Engineers' Handbook*, New York, McGraw-Hill Book Co., Inc., 1943. (On pp. 35-36, gives incorrect value for skin resistance of square wire by misuse of approximate formula from reference 1 above.)
5. H. A. Wheeler, "Universal Skin-Effect Chart for Conducting Materials," *Electronics*, Vol. 25, (November, 1952), pp. 152-154. (Various formulas for skin depth.)
6. H. A. Wheeler, "Conformal Mapping of Fields—Outline," *Wheeler Labs. Report 632*, July 7, 1923. (Includes outline of polygon rule.)
7. S. B. Cohn, "Problems in Strip Transmission Lines," *Symposium on Microwave Strip Circuits*, Tufts College, Medford, Mass., October, 1954. (Skin effect in certain polygon cross sections evaluated by incremental-inductance rule.)

## Active-Error Feedback and Its Application to a Specific Driver Circuit\*

J. R. MACDONALD†, SENIOR MEMBER, IRE

**Summary**—A short discussion of the advantages and disadvantages of active-error feedback in amplifier design is given. Such feedback can yield all the advantages of ordinary negative feedback without gain reduction and is particularly suitable for use in reducing the distortion of individual amplifier stages.

Active-error feedback is applied to a cathode follower by amplifying the difference between its input and output voltages, then adding the amplified error to the output. The resulting driver has very low output impedance and low distortion and is especially useful for driving the grid of an output tube far positive. A direct-coupled version of the circuit using ordinary miniature tubes had an output impedance of 5.6 ohms and could supply several hundred milliamperes of positive current. The theory of the circuit agrees with experiment, and the distortion of the driver when driving an output tube grid to the diode line is found to be far less than that of an ordinary cathode-follower driver.

\* Original manuscript received by the IRE, December 9, 1954; revised manuscript received, March 18, 1955.

† Texas Instruments Inc., 6000 Lemmon Avenue, Dallas 9, Texas.

### I. ACTIVE-ERROR FEEDBACK

UNLIKE ORDINARY negative feedback, where a portion of the available gain of an amplifier is expended in obtaining the benefits of feedback, active-error feedback (AEF) is a type of feedback with which no such direct gain reduction occurs. With AEF, a portion of the output signal from an amplifier or single-amplifier stage is subtracted from the input signal, then the resulting difference amplified in an external circuit whose gain is equivalent to the extra gain necessary with ordinary feedback. If the portion of the output subtracted is nominally equal to the input, the difference is proportional to the error or distortion in the output. This error is then injected back into the original circuit with the proper polarity to reduce the output error. Although the principle of AEF has been used in servomechanisms, it does not seem to have been as fully ex-

ploited in amplifier design as it deserves to be.<sup>1</sup> Therefore, it is worthwhile to discuss its advantages and disadvantages in this application in some detail and to present a specific example of this type of feedback.

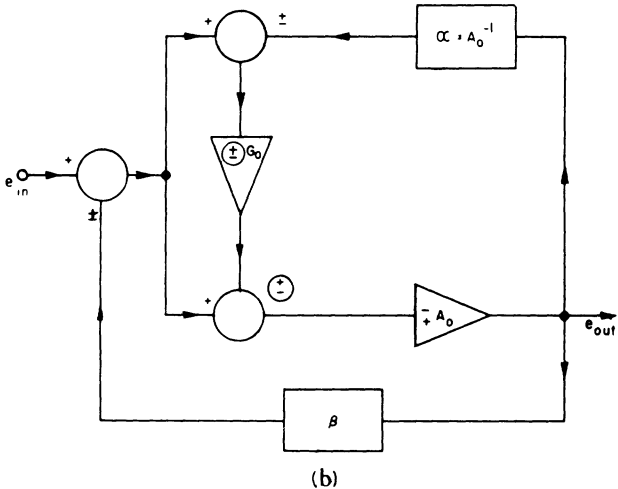
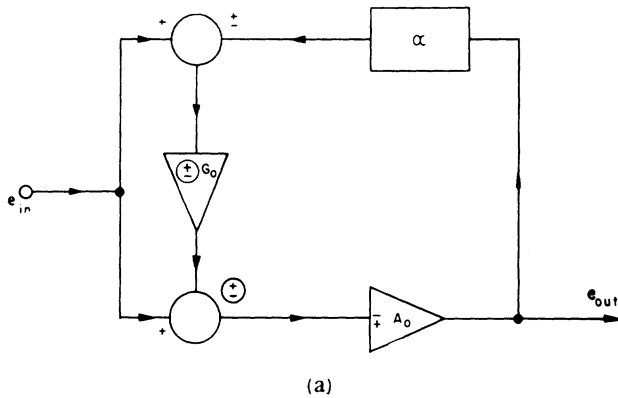
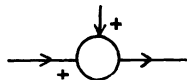


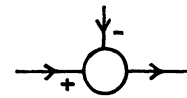
Fig. 1—(a) Block diagram showing connection of active error feedback around the amplifier of gain  $A_0$ ; (b) block diagram showing a method of combining active error feedback and ordinary negative feedback.

Fig. 1(a) shows a block diagram of a general AEF circuit. The circuit, the gain of which is to be stabilized, the distortion and output impedance of which are to be reduced, and the frequency response of which is to be improved, has a mid-frequency numerical gain of  $A_0$ . We have drawn this block diagram in terms of the positive mid-frequency numerical gains  $A_0$  and  $G_0$  rather than the complex phasor gains  $A(f)$  and  $G(f)$  in order to show explicitly the possible signs which may occur in the mid-frequency region. The symbol



indicates addition and

<sup>1</sup> F. E. Terman, "Radio Engineers' Handbook," McGraw-Hill Book Co., Inc., New York, pp. 403-404; 1943.



subtraction of the two input voltages. A variable voltage entering the junction at a plus sign goes through unchanged in sign, but a voltage entering at a minus sign has its polarity inverted. The plus-or-minus signs within circles in Fig. 1(a) go together as do those without circles, but the signs of the two sets may be specified independently.

The block diagram shows that the output voltage is multiplied by a factor  $\alpha$ , the result subtracted from the input voltage, and the resulting error voltage amplified by the factor  $G_0$ . Since only error voltage is amplified in this branch of the circuit, the amplifier of mid-band gain  $G_0$  need handle only fairly small signals and need not itself be distortionless. Finally the amplified error voltage is added to the input in such a phase sense that it reduces the difference between the input and  $\alpha$  times the output. It is usually most convenient to make  $\alpha$  the pure numeric  $A_0^{-1}$ . Then the AEF tends to make the output follow the input with no gain reduction.

Analysis of the block diagram yields the following result for the over-all gain  $e_{out}/e_{in}$ ,

$$e_{out}/e_{in} = A_0 [1 + G_0] / [1 + \alpha A_0 G_0] = A_0. \quad (1)$$

The second equation follows on taking  $\alpha = A_0^{-1}$ . If we continue to take  $\alpha = A_0^{-1}$  and generalize (9) for complex phasor gains, we obtain

$$\frac{e_{out}}{e_{in}} = \frac{A(f) [1 + G(f)]}{1 + G(f)A(f)/A_0}. \quad (2)$$

So long as  $G(f)A(f)$  is considerably greater than  $A_0$ , (2) reduces closely to

$$\frac{e_{out}}{e_{in}} \cong A_0, \quad (2')$$

the midband gain. We thus see that AEF can considerably extend the flat response of the  $A$ -circuit provided that the frequency response of the  $G$ -circuit is initially the wider and that  $G_0$  is considerably larger than unity. A straightforward calculation also shows that harmonic components and the output impedance are each reduced by the factor  $|1 + G(f)A(f)/A_0|$ , which will be considerably greater than unity over the frequency range of interest. Finally, (2') shows that the fundamental-signal gain of the circuit is stabilized by the AEF circuit to the mid-frequency value when  $\alpha = A_0^{-1}$ . Thus, the circuit yields the usual advantages of negative voltage feedback without the usual decrease of gain. The additional gain required is of course supplied by the active  $G$ -circuit. As in any feedback circuit, it is necessary, in order to avoid regeneration, that  $G(f)A(f)/A_0$  become less than unity before the phase shift of the combination reaches 180 degrees. The usual Nyquist criterion for stability is applicable here with  $\beta$  given by  $-G(f)/A_0$ .

A combination of AEF and negative feedback can be

applied to an amplifier as shown in Fig. 1(b). However, analysis of this circuit shows that the combination acts as though the extra gain of the AEF were directly in the normal negative feedback loop. Thus, although the effective negative feedback is increased, the AEF has not appreciably simplified the problem of equalizing the amplifier and feedback paths to avoid regeneration and to achieve unconditional stability. This latter statement needs qualification in one way. Since the gain  $G$  is essentially outside the main amplification path, its phase and amplitude may be conveniently controlled without the necessity (which might arise with the same total gain used only with negative feedback) of having to equalize the gain  $A$  and possibly thereby reduce the effective feedback at high or low frequencies. In addition, if the entire circuit is to be direct coupled, the splitting of the effective feedback into two paths in the fashion of Fig. 1(b) will usually require a smaller dc supply voltage than would be needed had all the available gain been distributed serially in the direct amplification path. When a large amount of effective negative feedback is required, its realization in a direct-coupled amplifier with reduced supply voltages may be an important economic advantage.

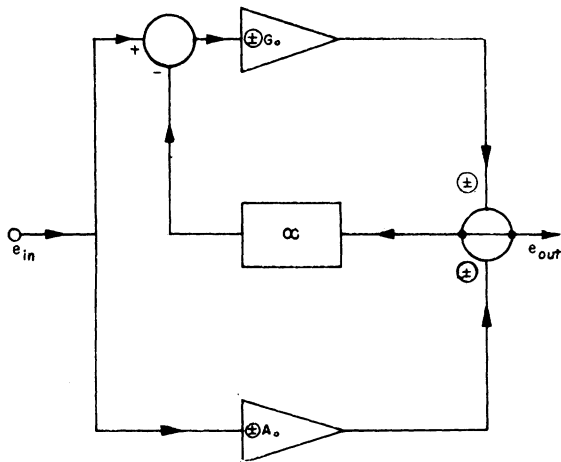


Fig. 2—Block diagram showing alternative connection of active error feedback.

The AEF circuit of Fig. 1(a) may be rearranged to inject the amplified error voltage into the output rather than the input of the amplifier of gain  $A(f)$ . The resulting circuit, with some of the possible signs indicated, is shown for midband gains in Fig. 2. If  $\alpha$  is taken as  $A_0^{-1}$  as usual, the complex gain of the circuit is found to be

$$\frac{e_{out}}{e_{in}} = A_0 \left[ \frac{A(f) + G(f)}{A_0 + G(f)} \right]. \quad (3)$$

Thus, the gain will be stabilized to the value  $A_0$  over a wide frequency range as long as  $G(f)$  is appreciably larger in magnitude than  $A(f)$ . Here it is necessary for stability that  $G(f)/A_0$  become less than unity before the phase shift of  $G(f)$  reaches 180 degrees.

The output impedances  $Z_A$  of amplifier  $A$  and  $Z_G$  of amplifier  $G$  will be connected together across the load in the circuit of Fig. 2. The effective output impedance of the combination (the internal impedance of the composite unit) is readily found to be

$$Z_{isff} = \frac{Z_A Z_G}{Z_G + Z_A [1 + G(f)/A_0]} \cong \frac{Z_G}{1 + G(f)/A_0}, \quad (4)$$

where the second equation follows when  $|G(f)|/A_0 \gg 1$  and when  $Z_G$  and  $Z_A$  are comparable. These conditions also lead to the gain given by (3).

When  $A_0$  is large, it will usually be inconvenient to make  $G_0/A_0 \gg 1$ . In this case, the AEF circuit of Fig. 1(a) will be more suitable than that of Fig. 2. However, when AEF is applied around an individual stage of relatively low gain, the circuit of Fig. 2 may become preferable. This may be particularly the case when added power or current handling capacity is required, since the  $A$  and  $G$  amplifier outputs are effectively in parallel and thus need each supply only part of the total required output power or current. Examples are a driver which must supply appreciable undistorted current, or a power output stage. The former will be discussed in more detail in the next section.

The distinction between amplified (or active) negative feedback and AEF should be emphasized. Amplified negative feedback would be obtained if the amplifier  $G$  amplified a portion  $\alpha$  of the output only. It is only when the error between a portion of the output and the input is amplified that AEF is obtained. It may be noted that amplified negative feedback produces the same reduction in output impedance that AEF does, but that while AEF stabilizes but does not reduce the midband gain, amplified negative feedback reduces it by about the same factor that the output impedance is reduced. It is obvious that while the present discussion has dealt only with AEF involving the output voltage, an AEF circuit could be applied which would make the output current, rather than the output voltage, follow the input voltage (or current).

## II. THE AUGMENTED CATHODE FOLLOWER

For many applications, a circuit having wide dynamic range and low output impedance is desirable. For example, the direct-coupled driver of an output tube which is to be driven into the positive-grid region must have such characteristics. The input resistance of such a tube may be as low as 100 ohms when its grid is driven far positive. Further, this resistance is a strongly nonlinear function of grid voltage. To avoid appreciable distortion, the driver of such a tube must itself have an output impedance considerably below 100 ohms and must, at the same time, be capable of supplying large positive peak grid currents.

An arbitrarily low output impedance can be obtained from an ordinary plate-loaded amplifier by applying sufficient negative voltage feedback around it. However,

the load current must flow through the output plate resistor, which is often undesirable, and the change of dc voltage level between the grid and plate of the output tube may complicate the use of such a circuit in a direct-coupled amplifier. Even if the driver tube itself is a cathode follower whose output impedance is reduced by ordinary inverse feedback around previous amplifier stages, these stages will be in the direct amplification path, again complicating its use in a direct-coupled circuit. In the present section, we show how these difficulties may be avoided by applying AEF to a cathode-follower driver. The resulting direct-coupled circuit has both very low output impedance and no appreciable change in dc voltage level between input and output.

Fig. 3 indicates one way of adapting the AEF circuit of Fig. 2 to a cathode follower. We shall call the resulting circuit a parallel augmented cathode-follower driver (PACFD). The type of AEF shown in Fig. 2 is particularly applicable to the cathode follower because the latter's gain is near unity and thus the external gain  $G$  need only be greater than unity to be effective in reducing output impedance and distortion. Further,  $\alpha$  can be conveniently taken equal to unity.

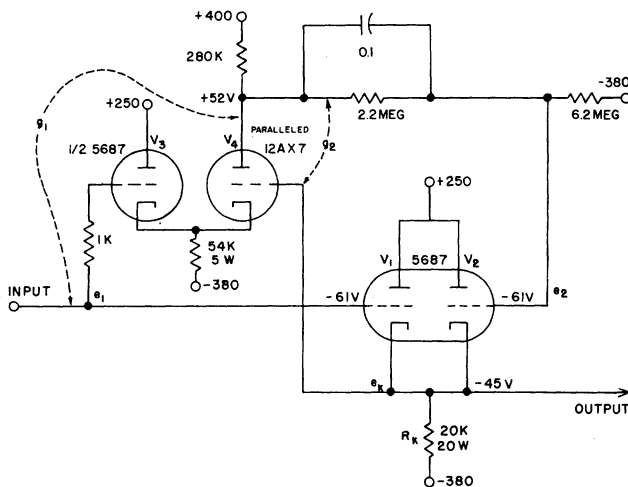


Fig. 3—The parallel augmented cathode-follower driver.

As shown in Fig. 3, the difference between the input  $e_1$  and the output  $e_k$  of tube  $V_1$  is amplified by the differential amplifier<sup>2</sup> consisting of  $V_3$  and  $V_4$ , then applied to the grid of the parallel cathode follower  $V_2$  to reduce the error between  $e_1$  and  $e_k$ . In this direct-coupled circuit, it is desirable that  $V_3$  be of the same tube type as  $V_1$  and  $V_2$ , in order that operating biases be correct. In an ac coupled version of the circuit both  $V_3$  and  $V_4$  could be, for example, the halves of a single 12AX7. It is worth mentioning that a cathode follower can be augmented in another way by using the tube half  $V_2$  as a cathode follower in series with  $V_1$  so that the cathode of

$V_2$  is connected to the plate of  $V_1$ . Then the grid of  $V_2$  could be direct-coupled to the plate of  $V_4$  without the voltage divider necessary in Fig. 3. We shall designate such a unit a series augmented cathode-follower driver (SACFD). The SACFD is superior to an ordinary cathode-follower driver (CFD) but inferior to a PACFD, as we shall see below. In addition, its dynamic range is limited, for a given supply voltage value, by the necessary voltage division across  $V_1$  and  $V_2$  in series, which does not occur with the PACFD.

A straightforward analysis of the midband equivalent circuits of the SACFD and PACFD yield the following results for their gains and internal impedances:

$$G_S = [\mu(1+g_1)+\mu^2]/[\mu g_2+(1+\mu)^2+(\mu+2)r_p/R_k], \quad (5)$$

$$r_{iS} = r_p/[\mu g_2/(2+\mu)+(1+\mu)^2/(2+\mu)+r_p/R_k], \quad (6)$$

$$G_P = \mu(1+g_1)/[\mu g_2+2(1+\mu)+r_p/R_k], \quad (7)$$

$$r_{iP} = r_p/[\mu g_2+2(1+\mu)+r_p/R_k]. \quad (8)$$

$G_S$  and  $r_{iS}$  refer to the SACFD,  $G_P$  and  $r_{iP}$  to the PACFD. In the above equations, the arithmetical gains  $g_1$  and  $g_2$  of the differential amplifier are those indicated on Fig. 1; they are slightly unequal, with  $g_2$  the larger. Note that the algebraic gain corresponding to  $g_2$  is negative.<sup>2</sup> It is also assumed that the tube halves  $V_1$  and  $V_2$  have the same characteristics. For most purposes, we shall ignore the small difference between  $g_1$  and  $g_2$  and designate them both by  $g$ . The above equations show that if  $\mu g$  is sufficiently large and  $r_p/R_k$  small, both  $G_S$  and  $G_P$  will approach unity closely. Further  $r_{iS}$  will approach  $r_p/(\mu+g)$  and  $r_{iP}$  will be approximately  $r_p/\mu g$ . Note that were amplified negative feedback used in the PACFD (e.g., by grounding the grid of  $V_3$  for input signals) instead of AEF,  $g_1$  would then be zero, and  $G_P$  would be reduced to about  $g_2^{-1}$  while  $r_{iP}$  would remain unchanged.

For comparison with the above results, the equations pertaining to an ordinary cathode follower are

$$G = \mu/[1 + \mu + r_p/R_k], \quad (9)$$

$$r_i = r_p/[1 + \mu + r_p/R_k]. \quad (10)$$

When  $r_p/R_k$  is small and  $\mu$  appreciably larger than unity, we see from these results that to good approximation the output impedance of the SACFD is reduced over that of an ordinary cathode follower of the same characteristics as  $V_1$  by the factor  $(\mu+g)/\mu$  and that of the PACFD is reduced by the factor  $g$ . The principal reason for the difference is that the error voltage at the plate of  $V_4$  is degenerated in the SACFD by a factor of about  $\mu$  when applied to the plate of  $V_1$  and so is less effective in reducing the output error than is that of the PACFD. Such degeneration is instrumental in reducing the dynamic range of the SACFD even further. Since the PACFD makes superior use of the same tubes required in the SACFD, we shall concentrate on the former in the rest of this work.

<sup>2</sup> G. E. Valley, Jr. and H. Wallman, "Vacuum Tube Amplifiers," Rad. Lab. Ser., McGraw-Hill Book Co., Inc., New York, vol. 18, pp. 442-443; 1948.

It may be noted that the double cathode follower<sup>3</sup> achieves, with two tubes in series, about the same small-signal gain and output impedance as the PACFD. The top input tube is plate loaded and its cathode connected to the plate of the bottom tube. The bottom tube is itself driven from the plate of the top tube. Neither the SACFD nor the double cathode follower are comparable to the PACFD as drivers, however. In the SACFD, the driving current must pass through both the upper series tube and the lower cathode-follower tube. In the double cathode follower, it must pass through both the load resistor  $R_L$ , which should be appreciably greater than  $r_p$ , and through the upper tube. In the PACFD, the driving current is supplied by both the cathode-followers  $V_1$  and  $V_2$  of Fig. 3, essentially in parallel. The dynamic range and current handling capacity of the PACFD are thus much superior to those of the other two circuits.

### III. COMPARISON OF THEORY AND EXPERIMENT

The circuit of Fig. 3 was constructed with the parameter values and tubes shown. It was found that its no-load gain was 0.986. Next, the output voltage was measured as a function of total load resistance  $R_L$  (the parallel combination of  $R_k$  and any added load) for a fixed input voltage. The measurements were carried out at  $10^4$  cps using a  $30 \mu f$  oil capacitor in series with a variable load resistance; only at the lowest load resistances was the capacitive reactance of importance.

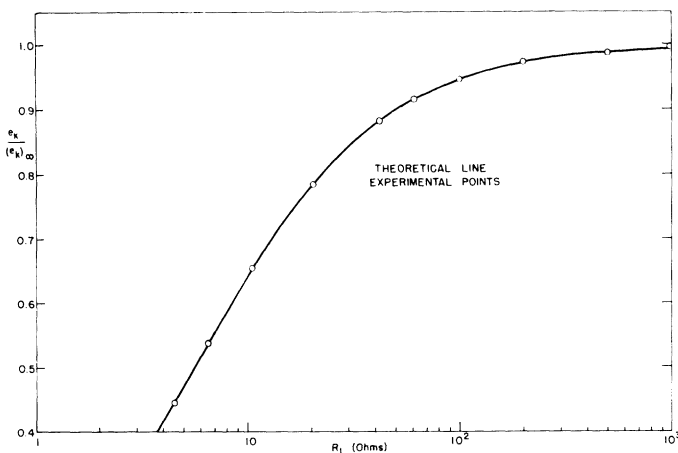


Fig. 4—Dependence on load resistance of the normalized output voltage of the PACFD.

Fig. 4 shows the load dependence of the output voltage  $e_k$  normalized with respect to that without load  $(e_k)_\infty$ . The theoretical line of this figure was calculated using (7) with  $R_k$  replaced by  $R_L$ . The values  $g = 70$ ,  $\mu = 16$  and  $r_p = 6.45$  kilohms were employed; these values are in reasonable agreement with published curves. Fig. 4 shows that these values are indeed a good choice, and that theory and experiment are in agreement. In addi-

tion, the internal impedance, defined as the added load necessary to make  $e_k / (e_k)_\infty = 0.5$ , is shown to be 5.6 ohms. For comparison, the internal impedances of the SACFD and CFD using the same tubes were found to be of the order of 70 and 370 ohms, respectively. The above definition of  $r_{iP}$  leads to the same result for this quantity as that given in (8), which was calculated on the basis of a grounded input and a measuring signal applied to the output. Alternatively, if  $r_{iP}$  is again determined by loading the output but defined as the added load required to make  $e_k / e_1 = 0.5$ , the expression for  $r_{iP}$  becomes

$$r_{iP} = r_p / [\mu(2g_1 - g_2) - 2 - r_p / R_k]. \quad (11)$$

For large  $\mu g$ , it does not differ appreciably from (8).

Next, the amplified error voltage  $e_2$  (see Fig. 3) was measured under the same conditions as above for a fixed input voltage  $e_1$ . The normalized quantity  $e_2 / e_1$  is plotted in Fig. 5 vs  $R_L$ . The small-signal equivalent circuit yields a value for this ratio of

$$\begin{aligned} e_2 / e_1 = & [\mu(2g_1 - g_2) \\ & + g_1(2 + r_p / R_k)] / [\mu g_2 + 2(1 + \mu) + r_p / R_k]. \end{aligned} \quad (12)$$

This quantity is slightly greater than unity even for  $R_k$  infinite. The solid line of Fig. 5 was calculated from (12), replacing  $R_k$  by  $R_L$  and using the same values for the tube parameters as those used for Fig. 4. Again, agreement between theory and experiment is exceptionally good. It is of interest to note that at very large loads  $e_2 / e_1$  may be much greater than unity; its maximum value will be approximately  $g$  if this value can be achieved without overdriving the tube  $V_4$ .

Finally, it should be pointed out that the data of Figs. 4 and 5 were measured with values of  $e_1$  of the order of 0.1 volt or less. The equivalent circuit and the resulting formulas only hold as long as operation is in a linear region. When negative peaks are to be produced across a load sufficiently large that the peak current required exceeds the quiescent current in  $R_k$ , the tubes  $V_1$  and  $V_2$  will be cut off and negative peak limiting will occur. Only by employing voltages sufficiently small that such limiting did not occur could an accurate undistorted value of  $e_k$  be obtained when very low load resistances were used. This negative peak limiting is the reason why a single PACFD or a pair in push-pull cannot be conveniently used to drive a load like a loudspeaker directly even though the small-signal impedances may be matched.

### IV. COMPARISON OF GRID-DRIVER CIRCUITS

The PACFD is ideally suited for a grid driver. Because it uses two cathode-followers essentially in parallel ( $V_1$  and  $V_2$ ), it can supply twice the peak positive grid current of a single unit. In addition, as the current increases, the  $g_m$  and  $\mu$  of both tubes increase and the  $r_p$ 's fall. For example, at 50 ma per tube-half, the  $\mu$  and  $g_m$  of a 5687 are approximately 19 and 12,000  $\mu$ mhos, re-

<sup>3</sup> S. Seely, "Electron-Tube Circuits," McGraw-Hill Book Co., Inc., New York, pp. 120-121; 1950.

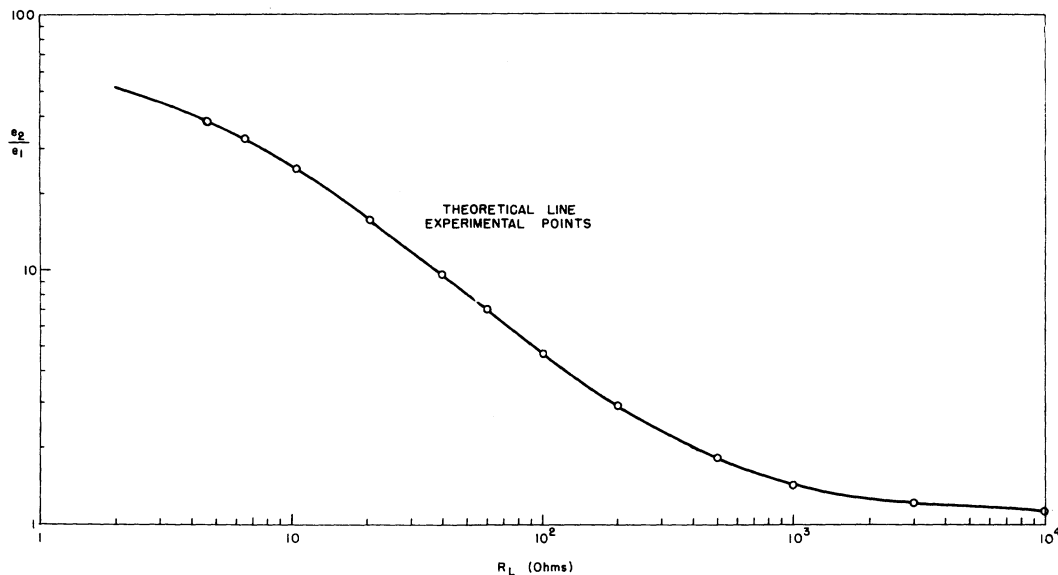


Fig. 5—Dependence on load resistance of the normalized error voltage of the PACFD.

spectively. Using  $g = 70$ , (8) or (11) predict an internal impedance of the PACFD of only about 1.15 ohms instead of the value of 5.6 ohms found for small signals with the circuit of Fig. 3.

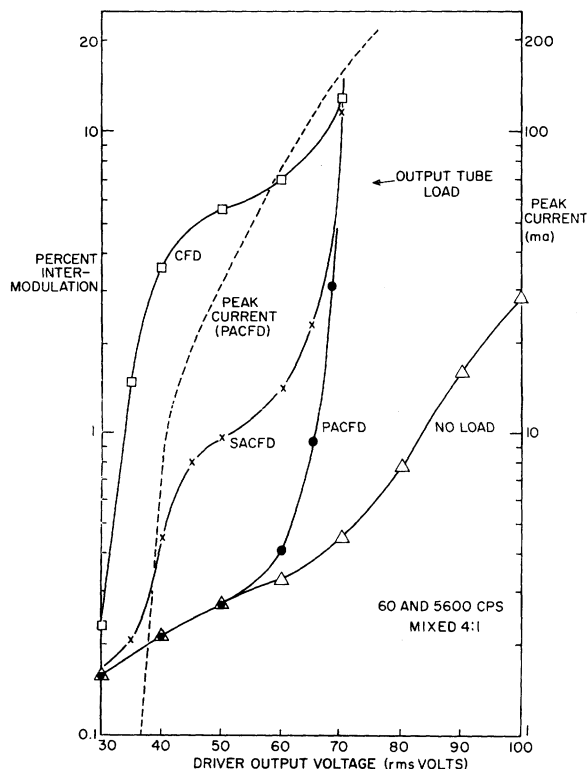


Fig. 6—Comparison between the intermodulation distortion of three drivers when direct-coupled to an output tube grid.

In Fig. 6, we give a comparison between the distortion generated by a CFD, a SACFD, and a PACFD when direct coupled to a power tube grid load. The lowest line, marked "no load," shows the distortion in the unloaded PACFD output. This distortion arises almost entirely from the preceding amplifier stage. The output tube

was an 807, triode connected, with 400 volts on the plate. It had an unbypassed 25-ohm cathode resistor and formed half of a push-pull output circuit with output transformer and resistive load. The other half of the push-pull output circuit was, in each case, driven by a driver identical to that measured.<sup>4</sup> The intermodulation distortion was measured at the output of the driver and employed 60 and 5,600 cps signals, mixed 4:1. The dc bias of the output tube was adjusted to  $-42.5$  volts so that the grid was driven positive when the rms driver voltage exceeded 30 volts. It is this positive grid region which is presented in Fig. 6.

The dotted line is the approximate peak grid current supplied by the driver. When the rms driver voltage is 70 volts, the grid is driven positive by 56.5 volts peak, and we see that it draws a peak current of about 200 ma. It is obvious from Fig. 6 that the SACFD is a considerable improvement on the CFD, and the PACFD an improvement on the SACFD over most of the range considered. For applied voltages greater than 60 to 65 volts rms, the grid of the output tube loses control of the output current on positive peaks; the point at which control is lost defines the diode line of the output tube. It is seen from the figure that the distortion of all the drivers increases rapidly for larger voltages. Oscillographic observations showed, however, that the PACFD was capable of driving the grid of the output tube considerably beyond the point where the output voltage of the output tube began to show peak clipping arising from diode-line limiting. Even in this region, however, appreciable distortion of the grid signal could not be observed on the CRO.

<sup>4</sup> The push-pull driver circuit used in these measurements incorporated a special feedback loop which reduced even-order harmonic distortion greatly at the driver outputs. Therefore, the intermodulation distortion results obtained at one of the push-pull driver outputs may be appreciably smaller, especially for the case of the CFD, than would be attained in practice without such a feedback loop. Nevertheless, the distortion curves still afford a valid comparison between the relative distortion of the three types of drivers.